Electronic Supplementary Material (ESI) for Sustainable Energy & Fuels.

Supporting Information

High Piezoresponse in Low-dimensional Inorganic Halide Perovskite for Mechanical Energy Harvesting

Aditi Sahoo[1], Tufan Paul[1], Nisha Hiralal Makani[1], Soumen Maiti[2], and Rupak Banerjee[1]*

[1]*Department of Physics, Indian Institute of Technology Gandhinagar, Palaj, Gandhinagar 382355, India*

[2] *St. Thomas Colleges of Engineering & Technology, Kolkata 700023, India*

*Corresponding author email: rupakb@iitgn.ac.in

Fabrication process of piezoelectric nanogenerator:

A PET substrate and an aluminium (Al) sheet (bottom electrode) were glued together to make a piezoelectric nanogenerator (PNG). The produced films were then deposited on the bottom Al electrode, which was then bonded to another Al sheet (top electrode). Two copper wires were attached to the top and bottom electrodes separately. PNG has an effective area of 10 cm^2. Following the approach described by Pusty et al. [1], the complete device is finally enclosed inside PDMS and further utilized for piezoelectric study.

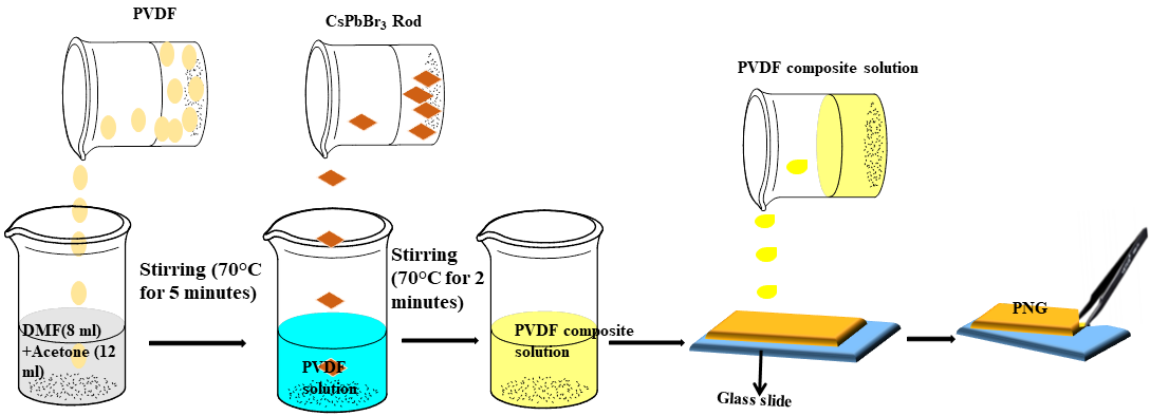

Figure S1: Schematic of 2D halide perovskite and PVDF composite preparation.

Figure S2: Digital image taken during film preparation and device encapsulation.

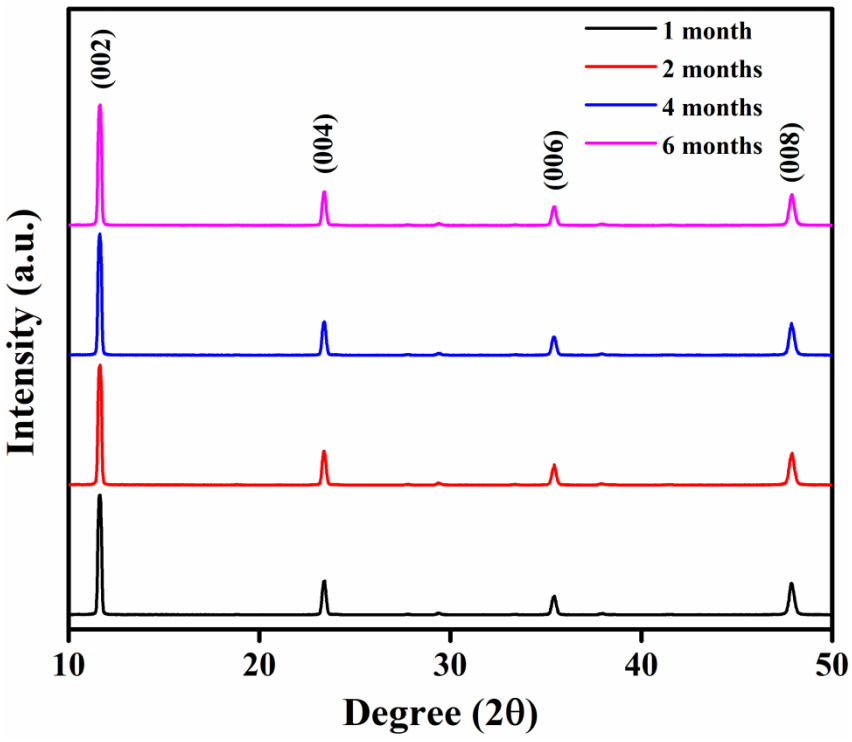

Figure S3: Time dependent XRD profile of the $CsPb_2Br_5$ sample.

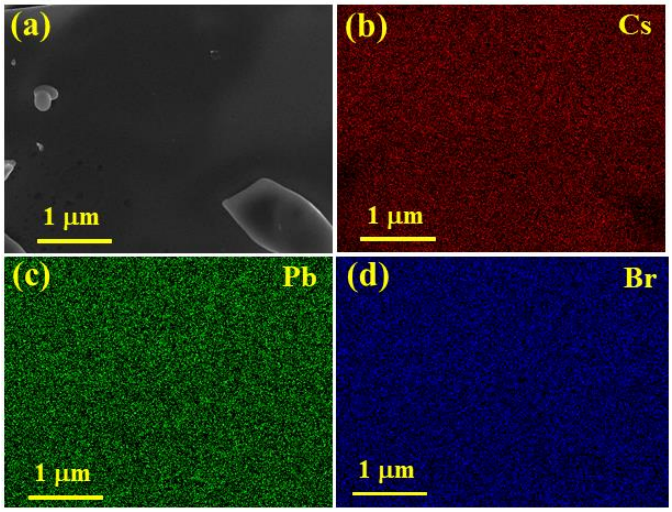

Figure S4: EDX elemental mapping of the $CsPb_2Br_5$ sample.

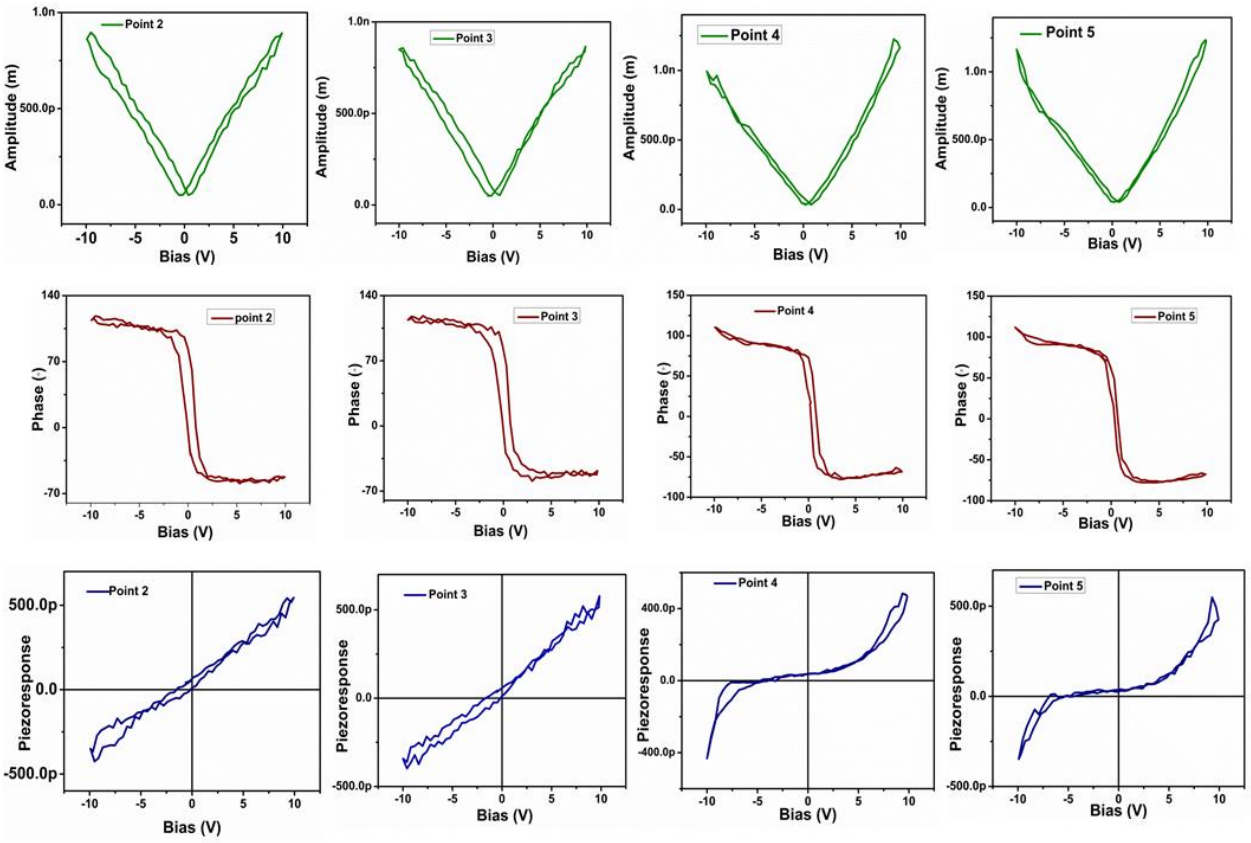

Figure S5: PFM response of the $CsPb_2Br_5$ sample at different locations.

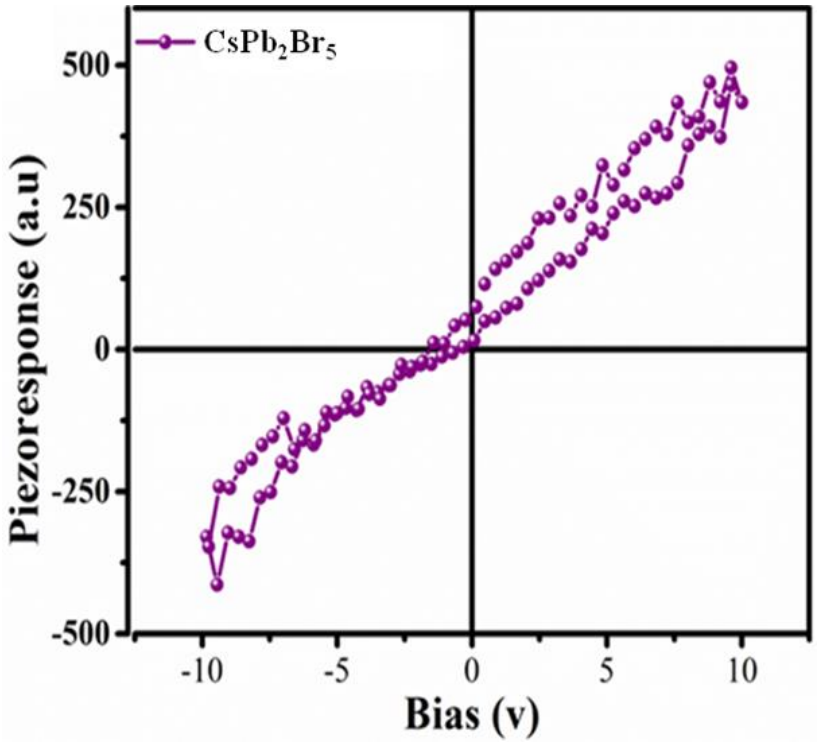

Figure S6: Piezoresponse loop of $CsPb_2Br_5$ microplate.

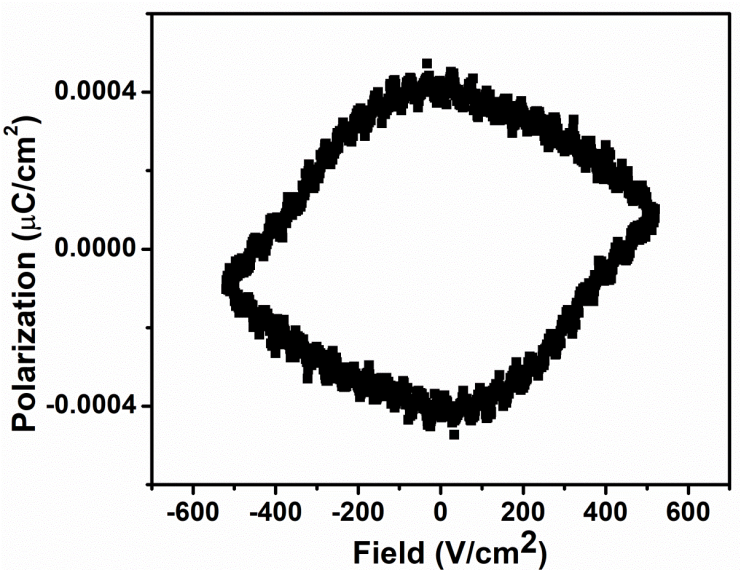

Figure S7: PE loop of the $CsPb_2Br_5$ sample.

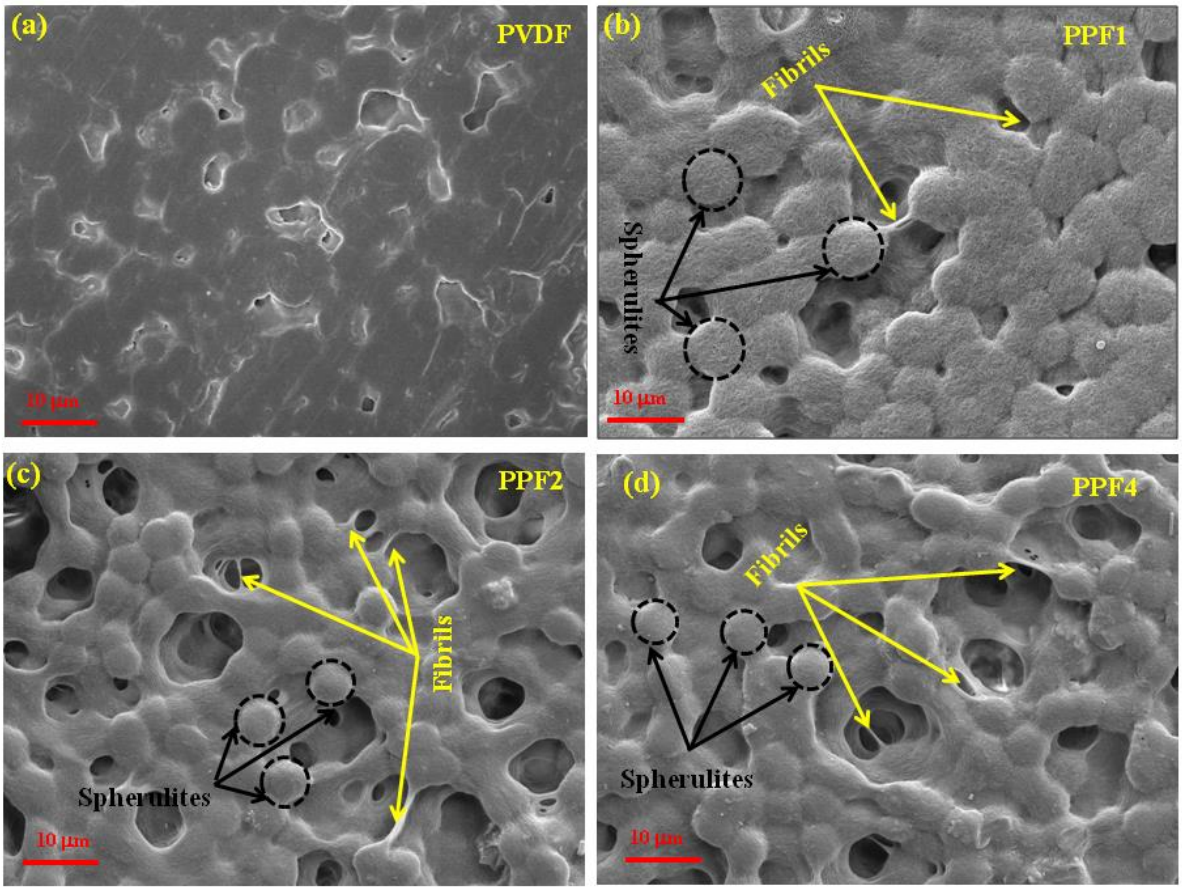

Figure S8: FESEM image of (a) pristine PVDF and $CsPb_2Br_5$-PVDF composites, (b) PPF1, (c) PPF2, and (d) PPF4.

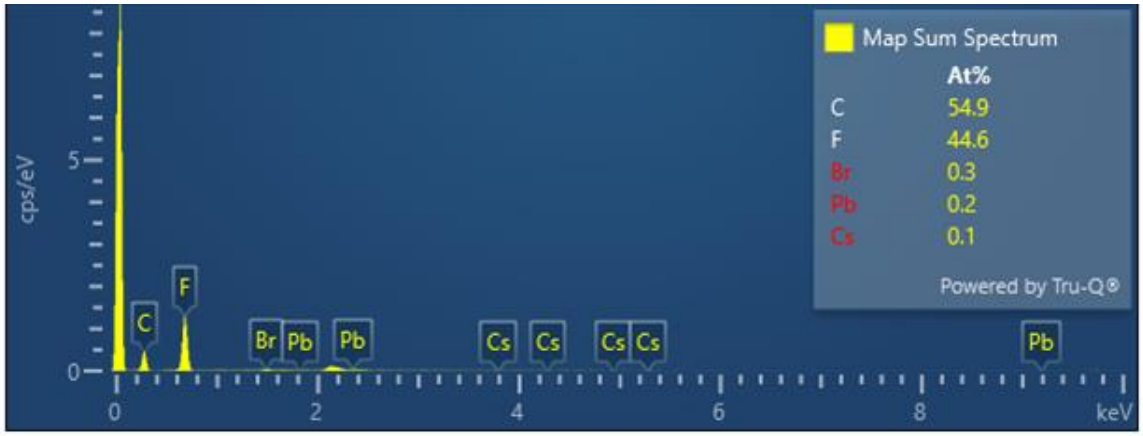

Figure S9: EDX spectrum of $CsPb_2Br_5$-PVDF composite of the PPF3 sample.

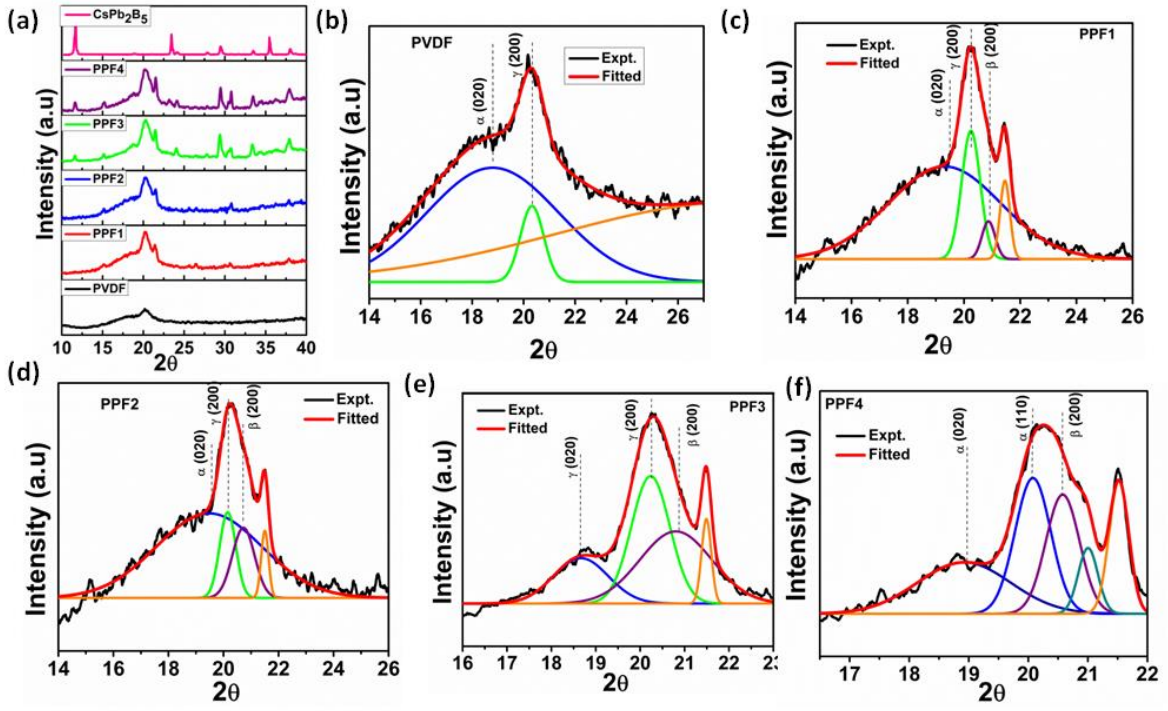

Figure S10: (a) XRD of PVDF and all the $CsPb_2Br_5$-PVDF composite films. (b) to (f) shows the deconvoluted peak profiles showing the peaks corresponding to the α, β and γ-phases in PVDF and all the $CsPb_2Br_5$-PVDF composite films.

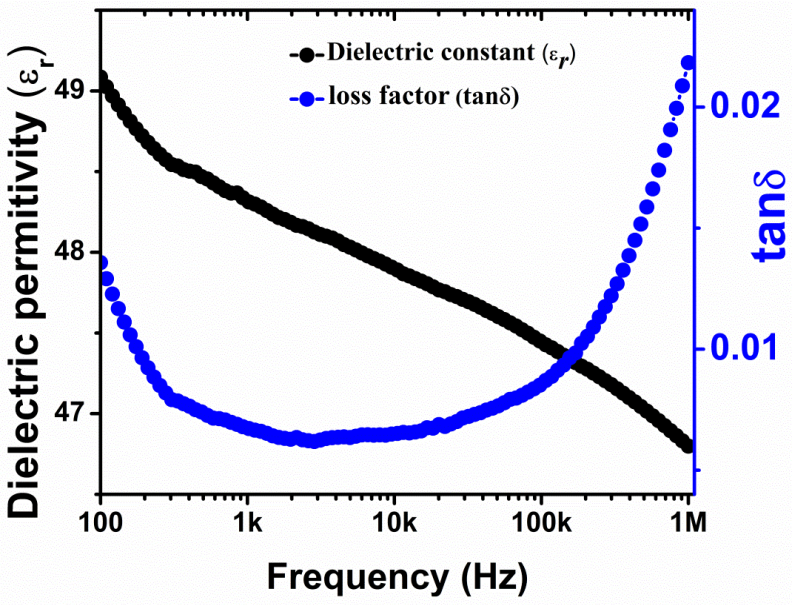

Figure S11: Frequency-dependent dielectric permittivity (ϵ_r) and loss factor (tanδ) of the PPF3 sample.

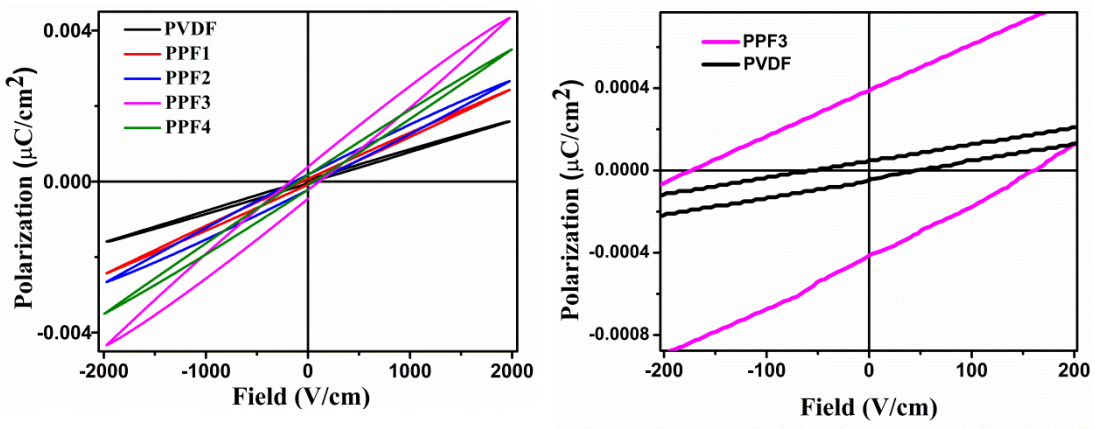

(a) (b)

Figure S12: (a) P-E loop for the pure PVDF and synthesized composites with different wt.% loading. (b) Enlarged view of P-E loop for PPF3 and PVDF for comparison.

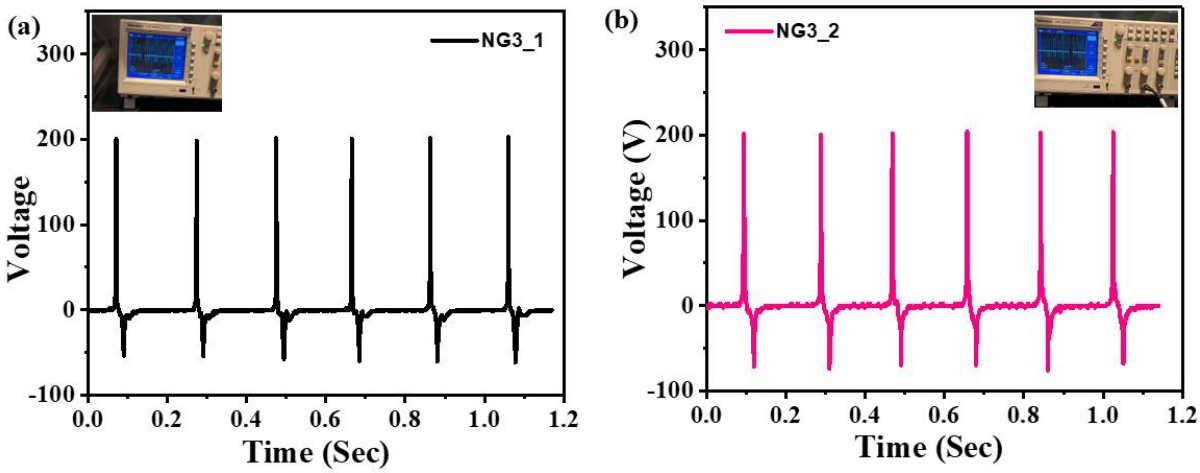

Figure S13: Output response from two different NG3 devices recorded at different times.

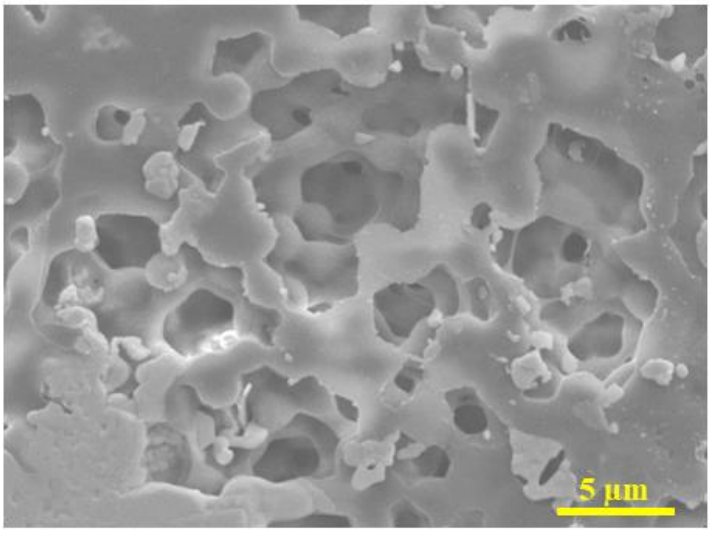

Figure S14: FESEM image of the composite film after a long 1000 cycle operation.

Table S1: Piezoelectric performance comparison

Device structure	**filler**	**Voltage (volt)**	**Current / current density**	**Power/power density**	**Stability cycle**	**Ref.**
PVDF with $CH_3NH_3PbBr_3$	$CH_3NH_3PbBr_3$	5	0.06 µA	-	3600	2
$FAPbBr_3$ -PDMS	$FAPbB_{r3}$	8.5	3.8 µA/cm^2	-	-	3
$FAPbBr_3$ -PVDF	$FAPbBr_3$	30	6.28 µA/cm^2	-	-	4
$MAPbI_3$ and PVDF	$MAPbI_3$	45.6	4.7 µA/cm^2.	-	-	5
PVDF/graphene	Graphene	20	-	-	125	6
ZnS/PDMS film	ZnS	35	-	2.43 µW/cm^3	-	7
PVDF/Al_2O_3 decorated rGO	Al_2O_3/rGO	36	0.8 µA	27.97 µW/cm3	1600	8
$ZnSnO_3$ and PDMS	$ZnSnO_3$	20	1µA/cm^2	-	-	9
BaTiO3 and graphitic carbons	PZT/MW-CNTs)	100	10µA	-	600	10
$CsPbBr_3$ (5%)-PVDF	$CsPbBr_3$	120 V	35 µA	4.24 mW	15000	11
$CsPb_2Br_5$ (3%) -PVDF	$CsPb_2Br_5$	**200 V**	**2.8 µA**	**120 µW**	**1000**	**This work**

References:

1. M. Pusty, L. Sinha and P. M. Shirage, New J. Chem., 43 (2019), 284.

2. A. Sultana, M. M. Alam, P. Sadhukhan, U. K. Ghorai, S. Das, T. R. Middya and D. Mandal, Nano Energy 49 (2018) 380-392.

3. R. Ding, H. Liu, X. Zhang, J. Xiao, R. Kishor, H. Sun, B. Zhu, G. Chen, F. Gao, X. Feng and J. Chen, Adv. Funct. Mater. 26 (2016) 7708-7716.

4. R. Ding, X. Zhang, G. Chen, H. Wang, R. Kishor, J. Xiao, F. Gao, K. Zeng, X. Chen, X.W. Sun and Y. Zheng, Nano Energy 37 (2017) 126-135.

5. V. Jella, S. Ippili, J. H. Eom, J. Choi and S. G. Yoon, Nano Energy 53 (2018) 46-56.

6. T. Huang, S. Yang, P. He, J. Sun, S. Zhang, D. Li, Y. Meng, J. Zhou, H. Tang, J. Liang and G. Ding, ACS appl. Mater. Interfaces. 10 (2018) 30732-30740.

7. A. Sultana, M. M. Alam, S. Garain, T. K. Sinha, T. R. Middya and D. Mandal, ACS Appl. Mater. Interfaces. 7 (2015) 19091-19097.

8. S. K. Karan, R. Bera, S. Paria, A. K. Das, S. Maiti, A. Maitra and B. B. Khatua, Adv. Energy Mater. 6 (2016) 1601016.

9. K. Y. Lee, D. Kim, J. H. Lee, T. Y. Kim, M. K. Gupta and S. W. Kim, Adv. Funct. Mater. 24 (2014) 37-43.

10. K. I. Park, C. K. Jeong, J. Ryu, G. T. Hwang and K. J. Lee, Adv. Energy Mater. 3 (2013) 1539-1544.

11. Suvankar Mondal, Tufan Paul, Soumen Maiti, Bikram Kumar Das, Kalyan Kumar Chattopadhyay, Nano Energy 74 (2020) 104870.